RESEARCH ARTICLE OPEN ACCESS

# Association of Spinal Cord Atrophy and Brain Paramagnetic Rim Lesions With Progression Independent of Relapse Activity in People With MS

Alessandro Cagol, MD, Pascal Benkert, PhD, Lester Melie-Garcia, PhD, Sabine A. Schaedelin, MSc, Selina Leber, MS, Charidimos Tsagkas, MD, PhD, Muhamed Barakovic, PhD, Riccardo Galbusera, MD, Po-Jui Lu, PhD, Matthias Weigel, PhD, Esther Ruberte, PhD, Ernst-Wilhelm Radue, MD, Özgür Yaldizli, MD, Johanna Oechtering, MD, Johannes Lorscheider, MD, Marcus D'Souza, MD, Bettina Fischer-Barnicol, MD, Stefanie Müller, MD, Lutz Achtnichts, MD, Jochen Vehoff, MD, Giulio Disanto, MD, PhD, Oliver Findling, MD, Andrew Chan, MD, Anke Salmen, MD, Caroline Pot, MD, PhD, Claire Bridel, MD, Chiara Zecca, MD, Tobias Derfuss, MD, Johanna M. Lieb, MD, Luca Remonda, MD, Franca Wagner, MD, Maria Isabel Vargas, MD, Renaud A. Du Pasquier, MD, Patrice H. Lalive, MD, Emanuele Pravatà, MD, Johannes Weber, MD, Philippe C. Cattin, PhD, Martina Absinta, MD, PhD, Claudio Gobbi, MD, David Leppert, MD, Ludwig Kappos, MD, Jens Kuhle, MD, PhD, and Cristina Granziera, MD, PhD

**Correspondence**
Dr. Granziera
cristina.granziera@usb.ch

*Neurology*® 2024;102:e207768. doi:10.1212/WNL.0000000000207768

## Abstract

### Background and Objectives

Progression independent of relapse activity (PIRA) is a crucial determinant of overall disability accumulation in multiple sclerosis (MS). Accelerated brain atrophy has been shown in patients experiencing PIRA. In this study, we assessed the relation between PIRA and neurodegenerative processes reflected by (1) longitudinal spinal cord atrophy and (2) brain paramagnetic rim lesions (PRLs). Besides, the same relationship was investigated in progressive MS (PMS). Last, we explored the value of cross-sectional brain and spinal cord volumetric measurements in predicting PIRA.

### Methods

From an ongoing multicentric cohort study, we selected patients with MS with (1) availability of a susceptibility-based MRI scan and (2) regular clinical and conventional MRI follow-up in the 4 years before the susceptibility-based MRI. Comparisons in spinal cord atrophy rates (explored with linear mixed-effect models) and PRL count (explored with negative binomial regression models) were performed between: (1) relapsing-remitting (RRMS) and PMS phenotypes and (2) patients experiencing PIRA and patients without confirmed disability accumulation (CDA) during follow-up (both considering the entire cohort and the subgroup of patients with RRMS). Associations between baseline MRI volumetric measurements and time to PIRA were explored with multivariable Cox regression analyses.

### Results

In total, 445 patients with MS (64.9% female; mean [SD] age at baseline 45.0 [11.4] years; 11.2% with PMS) were enrolled. Compared with patients with RRMS, those with PMS had accelerated cervical cord atrophy (mean difference in annual percentage volume change [MD-APC] −1.41; $p = 0.004$) and higher PRL load (incidence rate ratio [IRR] 1.93; $p = 0.005$). Increased spinal cord

RELATED ARTICLE

**Editorial**
Progression Independent of Relapse Activity in Multiple Sclerosis: Closer to Solving the Pathologic Puzzle
Page e207936

From Translational Imaging in Neurology (ThINk) Basel, Department of Biomedical Engineering, Faculty of Medicine (A. Cagol, L.M.-G., S.L., C.T., M.B., R.G., P.-J.L., M.W., E.R., E.-W.R., Ö.Y., L.K., C. Granziera), Neurologic Clinic and Policlinic, MS Center and Research Center for Clinical Neuroimmunology and Neuroscience Basel (RC2NB) (A. Cagol, L.M.-G., C.T., M.B., R.G., P.-J.L., M.W., E.R.,O.Y., J.O., J.L., M.D.S., B.F.-B., T.D., D.L., L.K., J.K., C. Granziera), Department of Clinical Research (P.B., S.A.S.), Division of Radiological Physics, Department of Radiology (M.W.), and Division of Diagnostic and Interventional Neuroradiology, Clinic for Radiology and Nuclear Medicine (J.M.L.), University Hospital Basel, University of Basel, Switzerland; Translational Neuroradiology Section (C.T), National Institute of Neurological Disorders and Stroke, National Institutes of Health (NIH), Bethesda, MD; Medical Image Analysis Center (MIAC) and Quantitative Biomedical Imaging Group (qbig), Department of Biomedical Engineering (E.R., P.C.C.), University Basel; Departments of Neurology (S.M., J.V.) and Radiology (J.W.), Cantonal Hospital St. Gallen; Departments of Neurology (L.A., O.F.) and Radiology (L.R.), Cantonal Hospital Aarau; Departments of Neurology (G.D., C.Z., C.G.) and Neuroradiology (E.P.), Neurocenter of Southern Switzerland, Lugano; Departments of Neurology, Inselspital (A. Chan, A.S.), and Diagnostic and Interventional Neuroradiology, Inselspital (F.W.) Bern University Hospital and University of Bern; Departments of Clinical Neurosciences, Division of Neurology (C.P., R.A.D.P.), and Radiology (R.A.D.P.) Lausanne University Hospital and University of Lausanne; Department of Clinical Neurosciences, Division of Neurology (C.B., P.H.L.), and Radiology (M.I.V.) Geneva University Hospitals and Faculty of Medicine; Faculty of Biomedical Sciences (C.Z.), Università della Svizzera Italiana, Lugano, Switzerland; Institute of Experimental Neurology, Division of Neuroscience (M.A.); Vita-Salute San Raffaele University and Hospital, Milan, Italy.

Go to Neurology.org/N for full disclosures. Funding information and disclosures deemed relevant by the authors, if any, are provided at the end of the article.

The Article Processing Charge was funded by Swiss National Fund.

## Glossary

**3D-EPI** = 3-dimensional echo planar imaging; **BPF** = brain parenchymal fraction; **CDA** = confirmed disability accumulation; **CSA** = cross-sectional area; **DMT** = disease modifying therapy; **EDSS** = Expanded Disability Status Scale; **FLAIR** = fluid-attenuated inversion recovery; **HR** = hazard ratio; **ICC** = intraclass correlation coefficient; **IRR** = incidence rate ratio; **MD-APC** = mean difference in annual percentage CSA change; **MPRAGE** = magnetization-prepared rapid gradient-echo; **MS** = multiple sclerosis; **PIRA** = progression independent of relapse activity; **PMS** = progressive MS; **PRL** = paramagnetic rim lesion; **QSM** = quantitative susceptibility mapping; **RAW** = relapse-associated worsening; **RRMS** = relapsing-remitting MS; **SMSC** = Swiss Multiple Sclerosis Cohort; **T2LV** = T2 lesion volume; **TIV** = total intracranial volume; **WML** = white matter lesion.

atrophy (MD-APC −1.39; $p = 0.0008$) and PRL burden (IRR 1.95; $p = 0.0008$) were measured in patients with PIRA compared with patients without CDA; such differences were also confirmed when restricting the analysis to patients with RRMS. Baseline volumetric measurements of the cervical cord, whole brain, and cerebral cortex significantly predicted time to PIRA (all $p \leq 0.002$).

### Discussion

Our results show that PIRA is associated with both increased spinal cord atrophy and PRL burden, and this association is evident also in patients with RRMS. These findings further point to the need to develop targeted treatment strategies for PIRA to prevent irreversible neuroaxonal loss and optimize long-term outcomes of patients with MS.

## Introduction

Multiple sclerosis (MS) is a chronic inflammatory, demyelinating, and neurodegenerative disease of the CNS, which represents the most frequent cause of nontraumatic disability in young adults.[1] The accumulation of disability in MS may either occur as a consequence of incomplete recovery from relapses (i.e., relapse-associated worsening [RAW]) or of progression independent of relapse activity (PIRA).[2] While PIRA is typical of the progressive forms of MS, there is increasing evidence that it can also present early in the disease course, affecting patients with a typical relapsing-remitting MS (RRMS) phenotype.[3-6] Notably, even in patients with RRMS, PIRA has been shown to constitute a critical determinant of overall disability accumulation.[4-6]

Different than the pathophysiology of relapses, the mechanisms underlying PIRA are only partially understood. We have previously described the involvement of diffuse neurodegenerative processes in patients with PIRA, reflected by accelerated brain atrophy.[7] It is plausible to hypothesize that spinal cord atrophy might also be related to the development of PIRA. Indeed, spinal cord atrophy has been previously shown to represent a strong predictor of physical disability and disease progression in MS[8,9]; moreover, accelerated cervical spinal cord atrophy has been recently reported in a mixed group of patients with RRMS and progressive MS (PMS) exhibiting "silent" clinical progression.[10]

The presence of focal chronic inflammatory activity in patients with MS might also be well-associated with the development of PIRA events. Indeed, chronic active lesions are known to cause smoldering demyelination and axonal injury in both the lesional and perilesional tissue,[11-13] likely contributing to disability accumulation. Notably, a subset of chronic active lesions can be detected in vivo on susceptibility-based MRI images through the identification of a rim of paramagnetic signal.[12,13] Paramagnetic rim lesions (PRLs) have been shown to constitute a negative prognostic biomarker in MS, being associated with more aggressive disease course.[13]

The aim of our study was to investigate whether ongoing degeneration in the spinal cord or the presence of focal smoldering inflammatory activity (PRLs) is associated with PIRA. Identifying mechanisms of neurodegeneration in PIRA will in fact enable not only the development of targeted treatments for patients with PIRA but also to better stratify them for the most appropriate therapeutic regimen. To achieve this goal, we studied a large multicentric cohort and explored the following:

1. The association between longitudinal rates of spinal cord atrophy and the occurrence of PIRA
2. The performance of cross-sectional brain and spinal cord volumetric measurements in predicting future evolution to PIRA
3. The association between the burden of brain PRLs and PIRA[12,13]

In addition, spinal cord atrophy and PRL burden were compared between patients with PMS and patients with RRMS.

## Methods

### Participants

From the Swiss Multiple Sclerosis Cohort (SMSC)—an observational multicentric study with standardized collection of clinical and MRI data[14]—we enrolled all patients with (1) diagnosis of MS according to the 2017 revisions of McDonald criteria[15]; (2) availability of an MRI scan including 3-dimensional echo planar

imaging (3D-EPI); (3) availability of regular clinical/conventional MRI follow-up in the 4 years preceding the 3D-EPI scan; and (4) age between 18 and 80 years. All patients participating in the SMSC between January 2012 and March 2022 were enrolled in the study if meeting the inclusion criteria.

The study follows the Strengthening the Reporting of Observational Studies in Epidemiology guideline for reporting observational studies.[16]

## Clinical Data

As part of the SMSC study, all patients underwent regular, standardized neurologic evaluations (performed at least annually), with the calculation of the Expanded Disability Status Scale (EDSS) score performed by certified raters.[17,18] The occurrence of relapses was recorded at each visit (further details are reported in eMethods 1, links.lww.com/WNL/D228). Confirmed disability accumulation (CDA) was determined as an increase in the EDSS score using a roving reference,[3] confirmed at least after 6 months, of (1) ≥1.5 points if baseline EDSS was 0; (2) ≥1.0 point if baseline EDSS was between 1.0 and 5.5; and (3) ≥0.5 points if baseline EDSS was greater than 5.5. Episodes of CDA occurring in the absence of relapses (1) between the EDSS increase and the precedent reference visit (performed at least 90 days before the EDSS increase) and (2) between the EDSS increase and the confirmation of disability progression were considered as PIRA.[7]

According to the clinical evolution during the 4-year follow-up preceding the 3D-EPI scan, we distinguished

1. Patients experiencing PIRA: presenting at least 1 episode of PIRA during the observation
2. Patients experiencing RAW: presenting at least 1 episode of CDA not fulfilling the criteria of PIRA
3. Patients without episodes of CDA during the entire follow-up

No patients experienced both PIRA and RAW during the observation.

## MRI Data

MRI scans were acquired at each center with protocols optimized for homogeneous signal-to-noise ratio (eTables 1 and 2, links.lww.com/WNL/D228).

We included all brain MRI scans performed as part of the SMSC study during the 4-year clinical follow-up. Those included 3D T1-weighted, 1-mm isotropic magnetization-prepared rapid gradient-echo (MPRAGE), covering also the upper cervical cord, and 3D 1-mm isotropic fluid-attenuated inversion recovery (FLAIR) images. An additional 3D-EPI acquisition was available at the end of the clinical follow-up for each patient; a concomitant post-contrast T1-weighted sequence was available for 93.3% of the patients.

## MRI Analysis

MRI analysis encompassed the following:

1. The quantification of longitudinal spinal cord atrophy rates, estimated by using all the available time points for each patient
2. The assessment of spinal cord and brain volumetric measurements at baseline (including exclusively the scans acquired ≤6 months from the beginning of clinical follow-up)
3. The detection of brain PRLs on susceptibility-weighted images, which were available for a single scan per patient (at the end of the clinical follow-up)

The study design is graphically summarized in Figure 1.

White matter lesions (WMLs) were automatically segmented,[19] and the results were manually reviewed. In patients with PIRA, the occurrence of new and enlarging lesions during follow-up was assessed by performing a longitudinal systematic comparison of all FLAIR images available during the observation period per each patient; automatic results[20] were manually reviewed.

For spinal cord morphological analysis, we measured the mean cross-sectional area (CSA) across C2-C3 vertebral levels using the DeepSeg algorithm from the Spinal Cord Toolbox (version 5.3.0),[21] using MPRAGE images as input. The C2-C3 intervertebral disk was manually labeled in each scan to ensure optimal placement, and all pipeline steps were manually reviewed.

Volumes of whole brain, thalamus, and cerebral cortex were obtained with SAMSEG (version 7.2.0),[22] after manual check of the reconstructions. The volumes were then normalized dividing by the total intracranial volume (TIV) to obtain the brain parenchymal fraction (BPF), thalamic fraction, and cortical fraction, respectively.

The presence of PRLs was assessed independently by 2 trained raters (A. Cagol; S.L.)—blinded to patients' identity—on both (1) unwrapped filtered phase and (2) quantitative susceptibility mapping (QSM).[23] PRLs were defined as discrete FLAIR hyperintense lesions either completely or partially surrounded by a rim of paramagnetic signal, clearly evident in at least 1 contrast between unwrapped phase and QSM (Figure 2). The chronic nature of PRLs was ensured by excluding all lesions showing gadolinium enhancement on postcontrast T1 images from the evaluation; for patients in whom contrast injection was not performed at the time of the 3D-EPI scan (6.7% of the cohort), PRLs were confirmed only if the corresponding lesions were present on a 3D-FLAIR image acquired ≥6 months prior.

## Statistical Analysis

The statistical analysis was conducted in R[24] and included the following:

1. Comparisons of baseline C2-C3 CSA between (1) patients with PMS and patients with RRMS

**Figure 1** Study Design

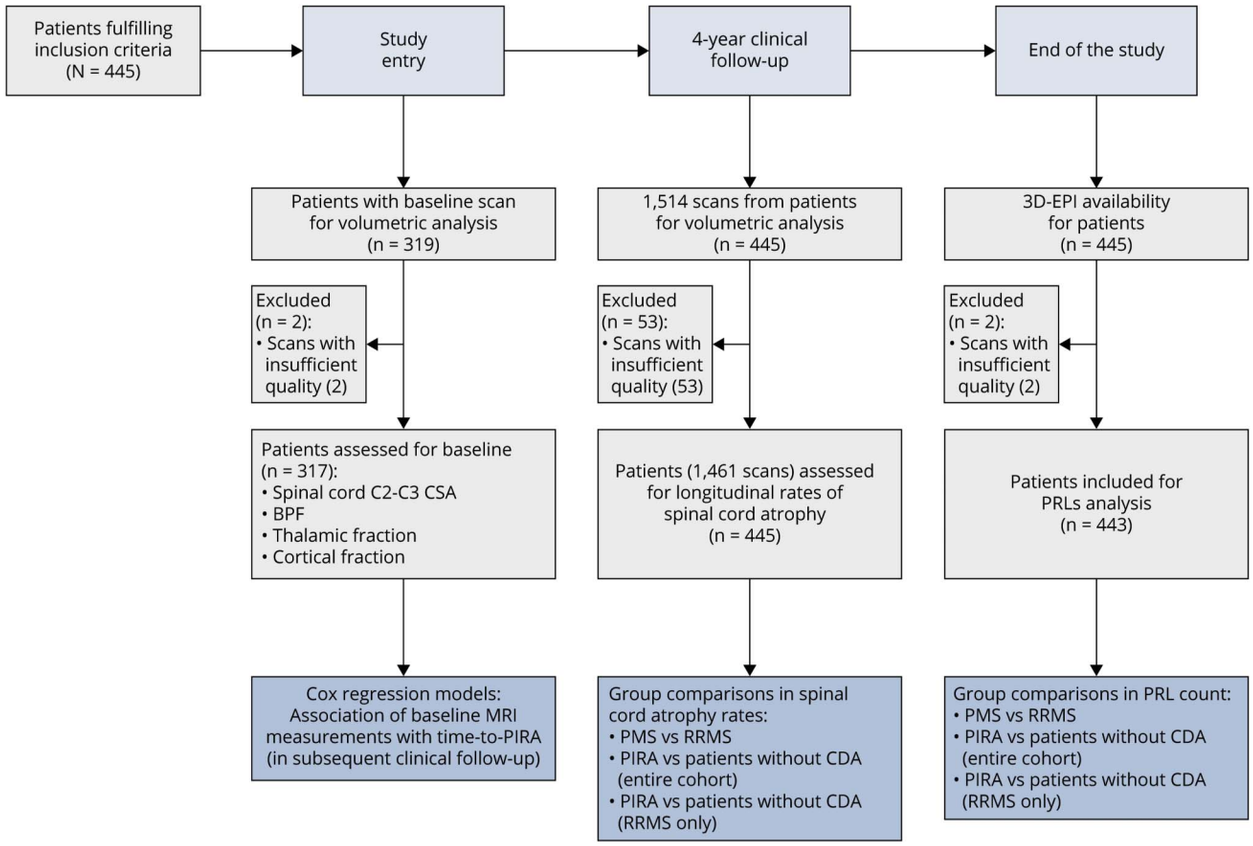


Baseline scans were considered the MRI scans acquired ≤6 months from the beginning of clinical follow-up. 3D-EPI = 3-dimensional echo planar imaging; BPF = brain parenchymal fraction; CSA = cross-sectional area; PIRA = progression independent of relapse activity; PMS = progressive multiple sclerosis; RRMS = relapsing-remitting multiple sclerosis.

and (2) patients who during follow-up developed PIRA and patients without CDA (considering both the entire cohort and patients with RRMS only). We used linear regression models with C2-C3 CSA as dependent variable and patient group as independent variable, adjusting for age, sex, disease duration, TIV, disease-modifying therapy (DMT) class, and MRI protocol. Further details are reported in eMethods 1 (links.lww.com/WNL/D228).

2. Investigation of longitudinal rates of cervical spinal cord atrophy with linear mixed-effect models,[25] using the C2-C3 CSA at each given time point as dependent variable. The CSA was log-transformed to quantify its annual percentage change from the slope over time. Models included patients and MRI protocol as

**Figure 2** Examples of PRLs in 2 Patients of the Cohort

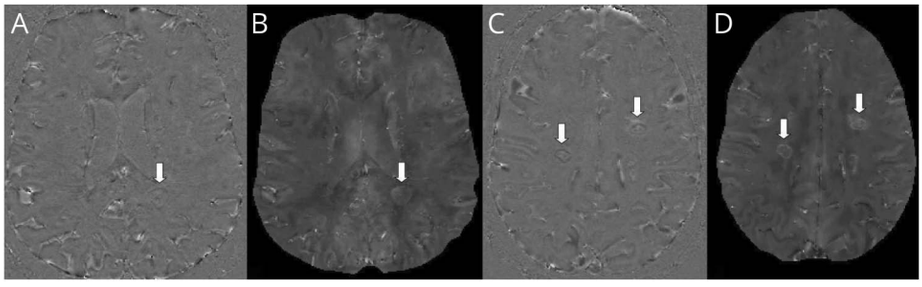


(A and C) Unwrapped-phase images and (B and D) quantitative susceptibility mapping images. PRLs are indicated by the arrows. PRL = paramagnetic rim lesion.

random intercepts, and a random slope on time. As fixed-effect covariates, we considered time, age at baseline, sex, disease duration at baseline, TIV, DMT class at baseline, and the interactions between age at baseline and sex with time. To compare the rates of spinal cord atrophy between patient groups, we introduced the interaction term between patient group and time in the abovementioned models. Effect size was expressed as mean difference in annual percentage CSA change (MD-APC). Rates of spinal cord atrophy were compared between (1) patients with PMS and patients with RRMS and (2) patients who during follow-up developed PIRA and patients without CDA (considering both the entire cohort and patients with RRMS only). As a sensitivity analysis, the comparison between patients with PIRA and patients without CDA was also performed after a 1:1 nearest neighbor propensity score matching of the groups, including age at baseline, sex, disease duration at baseline, DMTs class at baseline, and disease phenotype as criteria.

3. Multivariable Cox proportional hazards models to assess whether MRI measurements at baseline (namely, C2-C3 CSA, BPF, thalamic fraction, and cortical fraction) can predict time to PIRA. Age at baseline, sex, disease duration at baseline, DMTs class at baseline, and MRI protocol were included as covariates. Effect size was expressed in terms of hazard ratio (HR), and MRI measurements were scaled by subtracting the mean and dividing by the SD to obtain the HR per unit of SD change. Additional analyses on the predictive value of baseline MRI measurements on time to PIRA are reported in eAppendix 1 and eTable 3 (links.lww.com/WNL/D228).
4. Comparisons in PRL burden between (1) patients with PMS and patients with RRMS and (2) patients who during follow-up developed PIRA and patients without CDA (considering both the entire cohort and patients with RRMS only). Because of the overdispersed distribution of PRL count, between-group comparisons were explored with negative binomial regression models. Associations between PRL count and age, sex, disease duration, T2 lesion volume (T2LV), EDSS, and MS phenotype were explored in univariable negative binomial regression models. Effect size was expressed in terms of incidence rate ratio (IRR). Between-group comparisons in PRL burden were also explored using a cutoff of 2 PRLs per patients, as previously proposed by Maggi et al.[26] (eAppendix 2, eFigure 1, links.lww.com/WNL/D228). As sensitivity analysis, the comparison in PRL count between patients with PIRA and patients without CDA was also performed after a 1:1 nearest neighbor propensity score matching of the groups, including age, sex, disease duration, DMTs class, T2LV, and disease phenotype as criteria. Interrater agreement for PRL count was calculated with the intraclass correlation coefficient (ICC)[27].
5. Assessment of the relative strength of association between the occurrence of PIRA during follow-up (dependent variable) and (1) C2-C3 CSA and (2) PRL count (both measured on the same time-point and at the end of follow-up) in a multivariable logistic regression model (eAppendix 3, links.lww.com/WNL/D228).
6. Sensitivity analyses to exclude the potential confounding effect of focal inflammatory activity during follow-up on the estimation of spinal cord atrophy rates and PRL count. Specifically, between-group comparisons in spinal cord atrophy rates and PRL count were repeated after the exclusion of patients exhibiting relapse activity and subclinical radiologic activity.
7. Sensitivity analysis to assess the reproducibility of the association between PIRA and PRLs, exclusively considering patients with PIRA episodes that occurred less than 2 years before the PRL evaluation. Specifically, the comparison between patients experiencing PIRA less than 2 years before the PRL evaluation and patients without episodes of CDA was performed after a 1:1 nearest neighbor propensity score matching of the groups, including age, sex, disease duration, DMTs class, and disease phenotype as criteria.

Additional analyses, reported in the Supplementary material, include (1) the investigation of spinal cord atrophy and PRL burden in patients experiencing RAW during follow-up (eAppendix 4, links.lww.com/WNL/D228); (2) sensitivity analyses assessing potential bias resulting from the inclusion of heterogeneous MRI protocols (eAppendix 5); (3) sensitivity analyses excluding patients with primary progressive MS (eAppendix 6, eTables 4–7); and (4) cross-validation of the models investigating the rates of spinal cord atrophy and the predictors of time to PIRA to assess their generalization ability (eAppendix 7).

### Standard Protocol Approvals, Registrations, and Patient Consents

The study was approved by the local ethics committee (Ethikkommission Nordwest- und Zentralschweiz PB_2016-01171); written informed consent was obtained from all patients before study enrollment.

### Data Availability

The data that support the findings of this study may be available on reasonable request.

## Results

In total, 445 patients were included in the study; 2 patients had to be excluded from PRL analysis because of severe

artifacts in the 3D-EPI acquisition. For longitudinal spinal cord atrophy analysis, 1,514 MRI scans were available (53/1,514 discarded because of insufficient quality; no patients excluded). A baseline scan was available for 319 patients (2/319 excluded because of insufficient MRI quality). Examples of MRI images used for spinal cord atrophy and PRL assessment are provided in eFigures 2 and 3 (links.lww.com/WNL/D228).

During the 4-year follow-up, 74 patients presented PIRA episodes and 17 RAW episodes while the remaining 354 did not experience CDA. Table 1 summarizes the main clinical and MRI characteristics of the cohort; further details are available in eTables 8–10 (links.lww.com/WNL/D228).

## Spinal Cord CSA at Baseline

Compared with patients with RRMS, patients with PMS had smaller spinal cord C2-C3 CSA at baseline ($b$ = −4.628, 95% CI −7.483 to −1.773; $p$ = 0.002).

A lower spinal cord CSA was measured in patients that later during follow-up developed PIRA in comparison with patients who did not exhibit episodes of CDA ($b$ = −3.188, 95% CI −5.312 to −1.065; $p$ = 0.003). The same comparison, when restricted to patients with an RRMS phenotype, yielded similar results ($b$ = −2.678, 95% CI −5.112 to −0.245; $p$ = 0.031).

## Rates of Spinal Cord Atrophy

The annual rate of spinal cord atrophy in the entire cohort was −1.59% (95% CI −2.79 to −0.38).

When compared with patients with RRMS, patients with PMS presented with increased rates of spinal cord atrophy (MD-APC −1.41, 95% CI −2.36 to −0.47; $p$ = 0.004).

Patients experiencing PIRA during observation had increased rates of spinal cord atrophy in comparison with patients without CDA (MD-APC −1.39, 95% CI −2.18 to −0.59; $p$ = 0.0008). Similar results were obtained when performing the same comparison exclusively in patients with RRMS (MD-APC −1.22, 95% CI −2.17 to −0.27; $p$ = 0.013) (Figure 3).

After propensity score matching of patients with PIRA and patients without CDA, a significant difference in the rates of spinal cord atrophy was confirmed (MD-APC −1.40, 95% CI −2.41 to −0.40; $p$ = 0.007).

**Table 1** Clinical and MRI Characteristics in the Entire Cohort and in the Subgroups of Patients

| | Cohort (N = 445) | PIRA (n = 74) | RAW (n = 17) | Patients without CDA (n = 354) |
|---|---|---|---|---|
| **Baseline demographic and clinical data** | | | | |
| **Female, n (%)** | 289 (64.9) | 50 (67.6) | 12 (70.6) | 227 (64.1) |
| **Age, y, mean (SD)** | 45.0 (11.4) | 49.8 (11.8) | 41.3 (8.8) | 44.2 (11.2) |
| **Disease duration, y, median (IQR)** | 10.3 (5.7–17.9) | 14.7 (7.3–19.9) | 8.3 (3.8–14.3) | 9.4 (5.5–17.3) |
| **EDSS, median (IQR)** | 2.5 (1.5–3.5) | 3.0 (2.0–4.5) | 1.5 (1.0–2.0) | 2.0 (1.5–3.5) |
| **Disease course, n (%)** | | | | |
| **RRMS,** | 395 (88.8) | 49 (66.2) | 15 (88.2) | 331 (93.5) |
| **SPMS** | 36 (8.1) | 17 (23.0) | 2 (11.8) | 17 (4.8) |
| **PPMS** | 14 (3.1) | 8 (10.8) | 0 (0) | 6 (1.7) |
| **Patients on DMTs, n (%)** | 378 (84.9) | 58 (78.4) | 15 (88.2) | 305 (86.2) |
| **Platform, n** | 41 | 5 | 3 | 33 |
| **Oral, n** | 241 | 35 | 9 | 197 |
| **Monoclonal antibodies, n** | 96 | 18 | 3 | 75 |
| **Patients with relapse activity in the year before baseline, n (%)** | 14 (3.1) | 2 (2.7) | 1 (5.9) | 11 (3.1) |
| **Patients with relapse activity in the 2 y before baseline, n (%)** | 37 (8.3) | 5 (6.8) | 1 (5.9) | 31 (8.8) |
| **MRI data** | | | | |
| **MRI scans, n** | 1,514 | 251 | 70 | 1,193 |
| **No. of scans per patient, median (IQR)** | 4 (3–4) | 3 (3–4) | 4 (3–5) | 4 (3–4) |

Abbreviations: CDA = confirmed disability accumulation; DMT = disease modifying therapy; EDSS = Expanded Disability Status Scale; IQR = interquartile range; PIRA = progression independent of relapse activity; PPMS = primary progressive multiple sclerosis; RAW = relapse-associated worsening; RRMS = relapsing-remitting multiple sclerosis; SPMS = secondary progressive multiple sclerosis.

**Figure 3** Group Comparisons of Spinal Cord Atrophy Rates

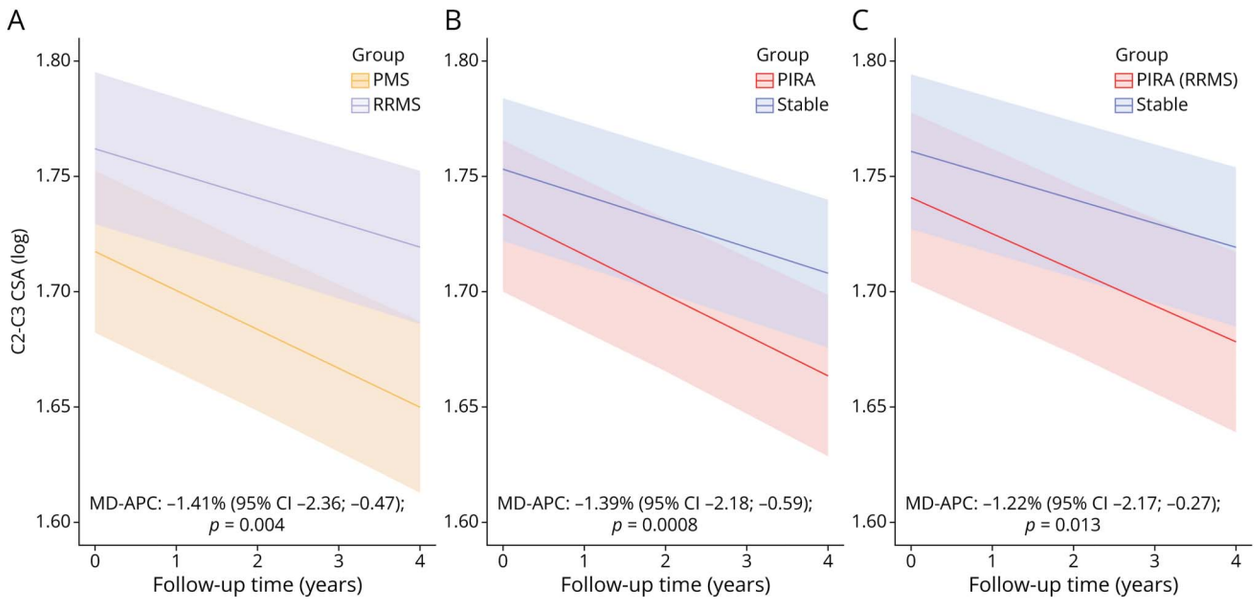


(A) Patients with PMS vs patients with RRMS, (B) patients experiencing PIRA during follow-up vs stable patients, and (C) patients experiencing PIRA during follow-up vs stable patients, considering exclusively patients with RRMS at baseline. The figures display predicted marginal effects from the multivariable mixed models. CSA = cross-sectional area; MD-APC = mean difference in annual C2-C3 cross-sectional area percentage change; PMS = progressive multiple sclerosis; PIRA = progression independent of relapse activity; RRMS = relapsing-remitting multiple sclerosis.

## Baseline MRI Measurements as Predictors of PIRA

Baseline C2-C3 CSA, BPF, and cortical fraction were all significant predictors of time to PIRA in multivariable Cox proportional hazard models while thalamic fraction was not. Specifically, the HR for time to PIRA of baseline C2-C3 CSA was 0.61 (95% CI 0.45–0.83; $p$ = 0.001), indicating an increase by 39% of the hazard of shorter time to PIRA for each SD decrease in C2-C3 CSA. The HR for time to PIRA was 0.59 (95% CI 0.43–0.82; $p$ = 0.002) for baseline BPF and 0.68 (95% CI 0.54–0.85; $p$ = 0.0008) for baseline cortical fraction (Figure 4).

Similar results were obtained when considering exclusively patients with RRMS at baseline, with HRs of 0.61 (95% CI 0.42–0.90; $p$ = 0.014) for baseline C2-C3 CSA, 0.63 (95% CI 0.42–0.94; $p$ = 0.024) for baseline BPF, and 0.60 (95% CI 0.39–0.91; $p$ = 0.015) for baseline cortical fraction.

Baseline C2-C3 CSA, BPF, and cortical fraction were also independent predictors of time to PIRA in models adjusted for the effect of T2LV (eAppendix 1, links.lww.com/WNL/D228). In a multivariable model including all the measures of brain and spinal cord atrophy considered (as well as T2LV), baseline C2-C3 CSA and cortical fraction remained significant independent predictors of time to PIRA (eAppendix 1).

## Paramagnetic Rim Lesions

Good interrater agreement in PRL detection was measured (ICC 0.91, 95% CI 0.90–0.93).

PRLs were detected in 64.8% of patients. The median (interquartile range) number of PRLs per patient in the cohort was 2 (0–6). The number of PRLs per patient was significantly associated with sex—with female patients presenting lower PRL count (IRR 0.72, 95% CI 0.53–0.97; $p$ = 0.032)—but not with age and disease duration. PRL count showed a positive association with T2LV (IRR 1.06, 95% CI 1.05–1.07; $p$ < 0.0001) and with the EDSS score (IRR 1.20, 95% CI 1.11–1.30; $p$ < 0.0001).

In comparison with the RRMS group, in the PMS group there was a higher PRL count (IRR 1.93, 95% CI 1.25–3.12; $p$ = 0.005). Patients developing PIRA during follow-up had higher PRL count than patients without episodes of CDA (IRR 1.95, 95% CI 1.34–2.92; $p$ = 0.0008). Similar results were found when restricting the analysis to patients with an RRMS disease course (IRR 1.72, 95% CI 1.10–2.85; $p$ = 0.025) (Figure 5).

After propensity score matching of patients with PIRA and patients without CDA, a significant difference in PRL count between groups was confirmed (IRR 1.62, 95% CI 1.07–2.46; $p$ = 0.021).

Between-group differences in PRL burden were also confirmed when using a 2-PRL cutoff to dichotomize patients (eAppendix 2, eFigure 1, links.lww.com/WNL/D228).

In the multivariable logistic regression model, PRL count and C2-C3 CSA were independently associated with the

**Figure 4** Survival Curves for Time to PIRA for Baseline Spinal Cord C2-C3 Cross sectional Area (A), Baseline Brain Parenchymal Fraction (B), Baseline Thalamic Fraction (C), and Baseline Cortical Fraction (D)

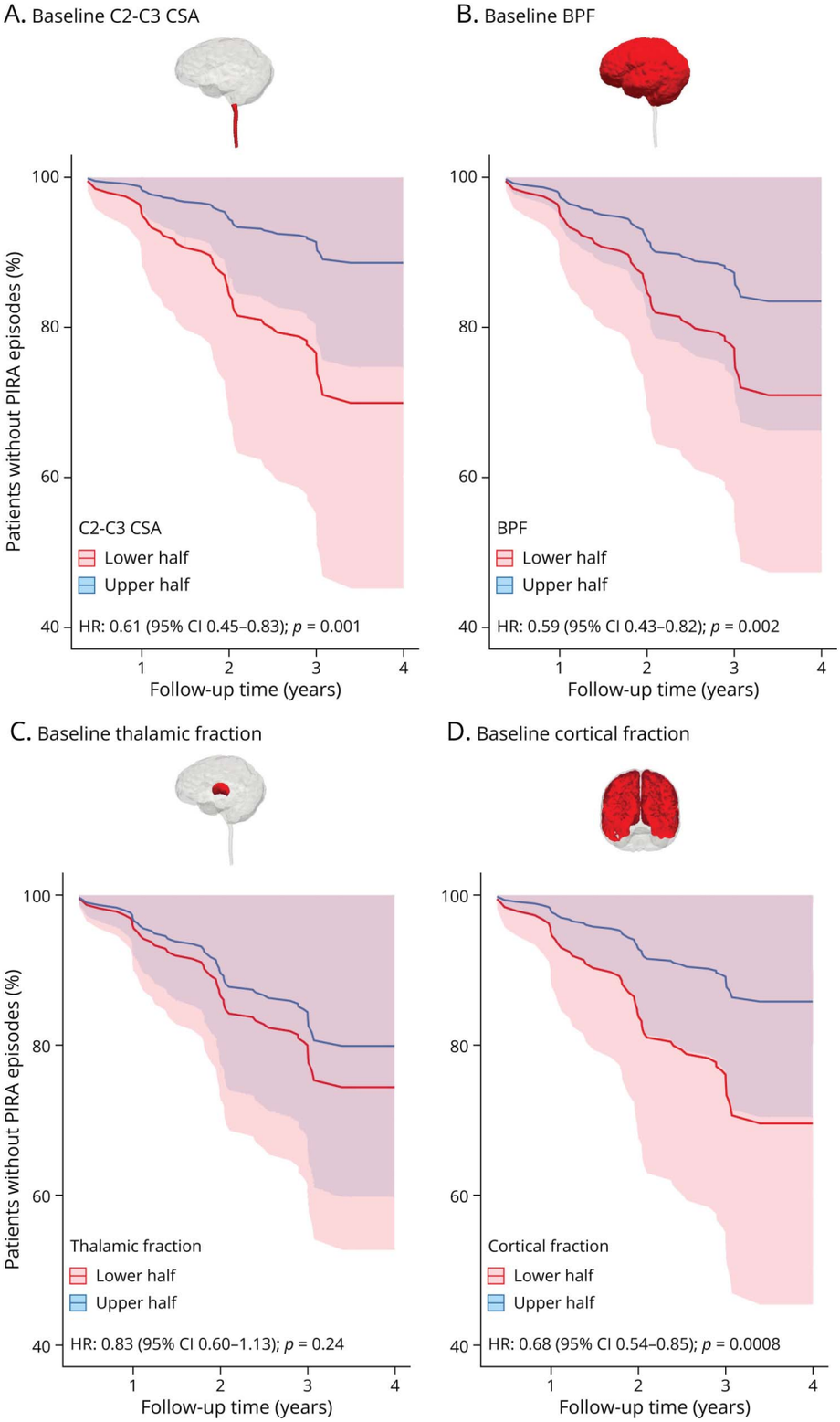


The curves display the longitudinal evolution in patients having baseline MRI measurements either higher ("upper half") or lower ("lower half") than the population average. Reported hazard ratio refers to the multivariable Cox regression models using baseline MRI measurements as continuous variables. BPF = brain parenchymal fraction; CSA = cross-sectional area; HR = hazard ratio; PIRA = progression independent of relapse activity.

**Figure 5** Group Comparisons of PRL Count

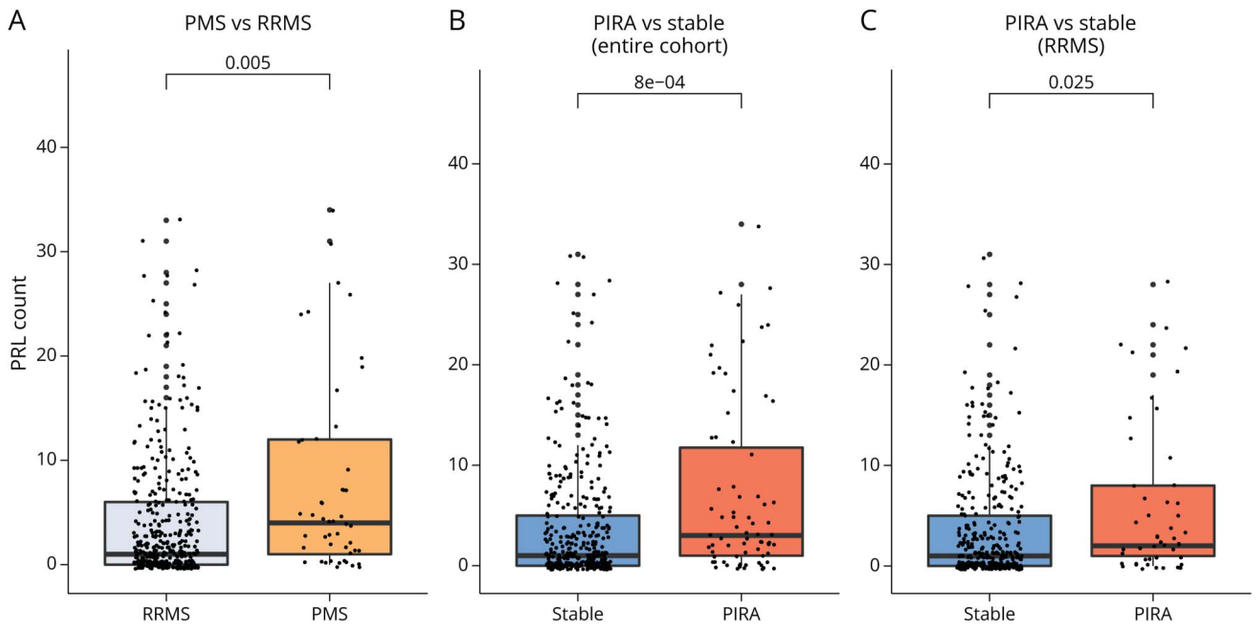


(A) Patients with PMS vs patients with RRMS, (B) patients experiencing PIRA during follow-up vs stable patients, and (C) patients experiencing PIRA during follow-up vs stable patients, considering exclusively patients with RRMS at baseline. The reported *p* values were obtained with univariable negative binomial regression models. PIRA = progression independent of relapse activity; PMS = progressive multiple sclerosis; PRL = paramagnetic rim lesion; RRMS = relapsing-remitting multiple sclerosis.

occurrence of PIRA during the 4-year follow-up (eAppendix 3, links.lww.com/WNL/D228).

### Sensitivity Analyses

In total, 4 patients with PMS and 63 patients with RRMS and 8 patients with PIRA and 59 patients without CDA experienced at least 1 relapse during follow-up. After their exclusion, the difference in spinal cord atrophy rates between patients with PMS and RRMS (MD-APC −1.51, 95% CI −2.51 to −0.53; $p = 0.003$) and between patients with PIRA and patients without CDA (MD-APC −1.19, 95% CI −2.02 to −0.36; $p = 0.006$) was confirmed.

Among the patients considered for PRL evaluation (443 of 445), 3 with PMS and 63 with RRMS and 8 with PIRA and 58 without CDA experienced relapse activity during follow-up. After their exclusion, the difference in PRL count between patients with PMS and RRMS patients (IRR 2.20, 95% CI 1.37–3.74; $p = 0.002$) and between patients with PIRA and patients without CDA (IRR 2.04, 95% CI 1.35–3.17; $p = 0.001$) remained significant.

When excluding patients with PIRA presenting either clinical relapses or new/enlarging WMLs during the entire follow-up (n = 17), a significant difference between patients with PIRA and patients without CDA was confirmed, both in terms of longitudinal spinal cord atrophy rates (MD-APC −1.13, 95% CI −2.02 to −0.23; $p = 0.015$), and PRL burden (IRR 2.19, 95% CI 1.40–3.58; $p = 0.001$).

A significant difference in PRL count between patients with PIRA and patients without CDA was also confirmed after restricting the analysis to patients with PIRA episodes that occurred less than 2 years before the PRL assessment (n = 33) (IRR 1.93, 95% CI 1.02–3.67; $p = 0.037$).

## Discussion

In this large, longitudinal cohort study, we found an association between PIRA and both diffuse and focal neurodegenerative processes, reflected by accelerated spinal cord tissue loss and higher burden of brain chronic active lesions. Indeed, increased spinal cord atrophy and PRL load were not only associated with PMS but were also evident in patients experiencing PIRA compared with patients without episodes of CDA. These results were also confirmed in patients exhibiting RRMS, further supporting the evidence that increased neuroaxonal loss can occur at all disease stages. Finally, we found that cross-sectional volumetric measures of the cervical spinal cord, brain, and cerebral cortex may serve as predictive biomarkers for PIRA. These results open new perspectives not only for the identification of targeted treatments for patients with PIRA but also for a better stratification of patients who will develop PIRA in the future, who might well deserve tailored therapeutic regimens.

When compared with patients without CDA during follow-up, patients experiencing PIRA had increased cervical cord

atrophy both cross-sectionally at baseline and longitudinally during follow-up. In patients with MS, spinal cord atrophy is typically extensive, reflecting both demyelination and neuroaxonal loss,[28] and it is evident already during the earliest disease phases.[29] Overall, the rates of cervical cord atrophy that we measured in this work are in line with previous studies investigating longitudinal upper cervical spinal cord area changes.[30] Our findings also corroborate the vast body of literature showing increased spinal cord atrophy in the progressive forms of MS, including both cross-sectional and longitudinal studies.[31] Several previous investigations have shown that spinal cord volume loss closely correlates with clinical disability[30,32,33] and constitutes a significant predictor of disease progression.[8,9] Our data show that the accumulation of disability occurring in the context of PIRA is associated with accelerated cervical cord tissue loss. Overall, our results are in line with a recent study,[10] where an accelerated cervical cord atrophy rate was described in relation to "silent" progression. Remarkably, although such a study used a novel procedure to quantify the upper cervical cord at C1 vertebral level, in our study, we considered the C2-C3 CSA as a measure of interest, which is more in line with the existing literature.[30] Moreover, in our work, we showed that cervical spinal cord atrophy is a phenomenon that also affects patients with PIRA in the RRMS phase, hereby extending previous results.[10]

In our study, both brain and spinal cord volumetric measurements at baseline proved to be relevant predictors of future evolution to PIRA, reflecting an increased risk of about 40% of shorter time to PIRA for each SD decrease. In addition, cortical gray matter volume was associated with time to PIRA, although this was not the case for thalamic volume in the multivariable model. These results are corroborating previous evidence reporting thalamic atrophy rates as relatively stable throughout the different stages of the disease,[34] as opposed to cortical atrophy, which tends to be accelerated in patients in the progressive phase of MS.[35,36] The implementation of longitudinal rates of brain and spinal cord atrophy as markers of disease progression in clinical practice is currently hampered by several biological and technical factors.[31,37] This considerably complicates the translation of the results obtained in large populations to the single-patient level.[31,37] On the other hand, here we show that the cross-sectional measurements of brain and spinal cord atrophy can qualify as predictors of PIRA, suggesting a path forward toward the implementation of personalized medicine approaches to identify patients at risk of PIRA in clinical practice.

We found higher load of PRLs in association with PIRA in both the entire cohort and the subgroup of patients with RRMS, reflecting an increased burden of focal chronic inflammatory activity and neurodegenerative processes. Overall, in our cohort, the PRLs were detected in 65% of patients. In comparison, previous studies have reported the presence of PRLs in 51.3% of patients with MS (pooled data from 31 MRI studies on 2,259 patients with MS),[38] albeit with high heterogeneity across studies.[39] With the aim of optimizing the sensitivity of detection of PRLs, in our work, we considered 2 MRI contrasts—unwrapped phase and QSM—which represent the most frequently used images for PRL detection.[39] The fact that in our cohort most patients presented PRLs is in line with previous MRI and pathologic studies, reporting glial-driven inflammation as a frequent phenomenon in MS despite concurrent treatment with DMTs.[11,13,40] Our results also confirm the positive association between PRL count and overall severity of disability.[13,41] The association between PRLs and both PMS and PIRA might be explained by the neurodegenerative processes that occur in chronic active lesions and the surrounding white matter. This would lead to substantial neuroaxonal loss, which represents the ultimate driver of irreversible disability.[42,43] Indeed, PRLs are associated with destructive processes involving the lesion core and periphery, including ongoing relentless damage in perilesional tissue.[13] Concordantly, previous longitudinal studies have found that PRL burden may serve as a marker of long-term clinical disability in MS, correlating with an increased likelihood of reaching higher motor and cognitive impairment and of transitioning to disease progression.[13,44] Moreover, the presence of PRLs has been associated with increased levels of serum neurofilament light chain, a marker of neuroaxonal loss, further corroborating the evidence of an association between PRLs and increased inflammatory-driven neurodegenerative processes.[26] The evidence that PRLs are associated with the occurrence of PIRA can be promising for potential applicability in patient monitoring. Because PRL detection has been shown to be comparable across field strengths (1.5 vs 3 T) using commercially available susceptibility-based sequences,[45] PRL evaluation might find substantial clinical utility in everyday practice in the near future.

This study has some limitations. First, the burden of PRLs was assessed only for a single time point for each patient, therefore not allowing the investigation of the temporal dynamics of the relationship between PRLs and PIRA. In addition, we defined a priori a 4-year period as a plausible time interval to assess the relationship between the occurrence of PIRA and the presence of PRLs, considering that the paramagnetic rim of PRLs proved to be stable over a few years.[12,13,46,47] Nevertheless, to at least partially address a potential bias derived by the chosen time-interval, we performed a sensitivity analysis restricting the time interval between PIRA occurrence and PRL evaluation to 2 years, which confirmed the results. Second, despite the acquisition protocol was standardized across centers, significant differences potentially affecting volumetric analyses were present because of the inclusion of MRI data obtained with heterogeneous MRI scanners and field strengths. We aimed to limit this confounding factor by systematically accounting for it in the statistical analyses. Third, we cannot completely exclude the possibility that subclinical cervical cord focal inflammatory activity may have partially influenced the observed rates of spinal cord atrophy. Fourth, because of the lack of measures of upper and lower extremity function in our cohort, subtle neurologic worsening without any effect on the EDSS score may have been overlooked.

In this study, we show that PIRA is associated with neurodegenerative processes in the spinal cord and with the presence

of brain chronic active lesions. Our results, together with previous evidence showing increased CNS structural damage in PIRA,[5,7,10,48] stress the need for early recognition of PIRA in clinical practice to prevent irreversible tissue loss. To this end, cross-sectional measures of brain and cervical spinal cord volume could be of value. In addition, this work is once more questioning the existence of a clear distinction between relapsing-remitting and progressive MS forms.[4,7,10,49] Indeed, accelerated neurodegeneration was not only identified in patients with PMS but also associated with PIRA in patients with RRMS. Therefore, our results add to the increasing evidence[4,5,7,10,49] proposing an interpretation of MS as a continuum of inflammatory and neurodegenerative processes, rather than a condition with distinct disease phenotypes reflecting different pathophysiologic substrates.

## Acknowledgment

We express our deep thankfulness to patients and relatives for their participation and support, study nurses in participating centers for their motivated collaboration and recruitment efforts, and the administrative personnel of the Swiss Multiple Sclerosis Cohort study.

## Study Funding

The Swiss MS Cohort study received funding from the Swiss MS Society and unrestricted grant funding from Biogen, Celgene, Merck, Novartis, Roche, and Sanofi.

## Disclosure

A. Cagol, P. Benkert, L. Melie-Garcia, S.A. Schaedelin, S. Leber, C. Tsagkas, M. Barakovic, R. Galbusera, and P.-J. Lu have nothing to disclose. M. Weigel is partially funded by Biogen for the development of spinal cord MRI for patients with spinal muscular atrophy. E. Ruberte and E.-W. Radue have nothing to disclose. Ö. Yaldizli received grants from ECTRIMS/MAGNIMS, University of Basel, Pro Patient Stiftung University Hospital Basel, Free Academy Basel, Swiss Multiple Sclerosis Society and advisory board/lecture and consultancy fees from Roche, Sanofi Genzyme, Allmirall, Biogen and Novartis. J. Oechtering received research support by the Swiss MS Society and served on advisory boards for Roche and Merck. J. Lorscheider has received research support from Innosuisse-Swiss Innovation Agency, Biogen and Novartis, and speaking honoraria and/or fees for serving on advisory boards from Novartis, Roche and Teva. M. D'Souza has nothing to disclose in relationship to this work. B. Fisher-Barnicol has nothing to disclose. S. Müller received honoraria for travel, honoraria for lectures/consulting, and/or grants for studies from Almirall, Biogen, Celgene, Novartis, Teva, Merck Serono, Genzyme, Roche, and Bayer Schweiz. L. Achtnichts has nothing to disclose. J. Vehoff received honoraria for travel, honoraria for lectures/consulting and/or grants for studies from Allmiral, Biogen, Novartis, Teva, Merck-Serono, Genzyme, Roche and Bayer Schweiz AG, none related to this work. G. Disanto and O. Findling have nothing to disclose. A. Chan has served on advisory boards for, and received funding for travel or speaker honoraria from, Actelion-Janssen, Almirall, Bayer, Biogen, Celgene, Sanofi-Genzyme, Merck, Novartis, Roche, and Teva, all for hospital research funds; and research support from Biogen, Genzyme and UCB. A. Chan is associate editor of the *European Journal of Neurology* and serves on the editorial board for *Clinical and Translational Neuroscience* and as topic editor for the *Journal of International Medical Research*. A. Salmen received speaker honoraria for activities with Bristol Myers Squibb, CSL Behring, Novartis, and Roche, and research support by the Baasch Medicus Foundation, the Medical Faculty of the University of Bern and the Swiss MS Society. All not related to this work. C. Pot and C. Bridel have nothing to disclose. C. Zecca institution the Department of Neurology, Regional Hospital Lugano (EOC), Lugano, Switzerland receives financial support from Teva, Merck Serono, Biogen, Genzyme, Roche, Celgene, Bayer and Novartis. T. Derfuss received speaker fees, research support, travel support, and/or served on Advisory Boards or Steering Committees of Actelion, Alexion, Biogen, Celgene, GeNeuro, MedDay, Merck, Mitsubishi Pharma, Novartis, Roche and Sanofi-Genzyme; he received research support from Alexion, Biogen, Novartis, Roche, Swiss National Research Foundation, University of Basel, and Swiss MS Society. J.M. Lieb, L. Remonda, F. Wagner, M.I. Vargas, and R. Du Pasquier have nothing to disclose in relationship to this work. P.H. Lalive received honoraria for speaking and or travel expense from Biogen, Merck, Novartis, Roche; consulting fees from Biogen, GeNeuro, Merck, Novartis, Roche; research support from Biogen, Merck, Novartis. None were related to this work. E. Pravatà, J. Weber, and P.C. Cattin have nothing to disclose. M. Absinta is supported by the Conrad N. Hilton Foundation (17313), the Cariplo Foundation (2019-1677), the FRRB Early Career Award (1750327) and the International Progressive MS Alliance (PA-2107-38081); she received consultancy fees from GSK and Abata Therapeutics unrelated to this work. C. Gobbi institution the Department of Neurology, Regional Hospital Lugano (EOC), Lugano, Switzerland received financial support from Teva, Merck Serono, Biogen, Genzyme, Roche, Celgene, Bayer and Novartis. PHL received honoraria for speaking from Biogen-Idec, CSL Bering, Merck Serono, Novartis, Sanofi-Aventis, Teva; consulting fees from Biogen-Idec, Geneuro, Genzyme, Merck Serono, Novartis, Sanofi-Aventis, Teva; research grants from Biogen-Idec, Merck Serono, Novartis. D. Leppert is Chief Medical Officer of GeNeuro. L. Kappos institution (University Hospital Basel) has received the following exclusively for research support: Steering committee, advisory board, and consultancy fees (Actelion, Bayer HealthCare, Biogen, BMS, Genzyme, Janssen, Merck, Novartis, Roche, Sanofi, Santhera, TG Therapeutics); speaker fees (Bayer HealthCare, Biogen, Merck, Novartis, Roche, and Sanofi); support of educational activities (Allergan, Bayer HealthCare, Biogen, CSL Behring, Desitin, Genzyme, Merck, Novartis, Roche, Pfizer, Sanofi, Shire, and Teva); license fees for Neurostatus products; and grants (Bayer HealthCare, Biogen, European Union, InnoSwiss, Merck, Novartis, Roche, Swiss MS Society, and Swiss National Research Foundation). J. Kuhle received speaker fees, research support, travel support, and/or served on advisory boards by

Swiss MS Society, Swiss National Research Foundation (320030_189140/1), University of Basel, Progressive MS Alliance, Bayer, Biogen, Celgene, Merck, Novartis, Octave Bioscience, Roche, Sanofi. C. Granziera: The University Hospital Basel (USB), as the employer of C.G., has received the following fees which were used exclusively for research support: (1) advisory board and consultancy fees from Actelion, Genzyme-Sanofi, Novartis, GeNeuro and Roche; (2) speaker fees from Genzyme-Sanofi, Novartis, GeNeuro and Roche; (3) research support from Siemens, GeNeuro, Roche. Go to Neurology.org/N for full disclosures.

## Publication History

Received by *Neurology* June 8, 2023. Accepted in final form September 18, 2023. Submitted and externally peer reviewed. The handling editor was Deputy Editor Olga Ciccarelli, MD, PhD, FRCP.

## Appendix Authors

| Name | Location | Contribution |
|---|---|---|
| **Alessandro Cagol, MD** | University of Basel | Drafting/revision of the manuscript for content, including medical writing for content; study concept or design; analysis or interpretation of data |
| **Pascal Benkert, PhD** | Clinical Trial Unit, University Hospital Basel | Drafting/revision of the manuscript for content, including medical writing for content; major role in the acquisition of data; analysis or interpretation of data |
| **Lester Melie-Garcia, PhD** | University of Basel | Drafting/revision of the manuscript for content, including medical writing for content; major role in the acquisition of data |
| **Sabine A. Schaedelin, MSc** | University Basel Hospital | Drafting/revision of the manuscript for content, including medical writing for content; analysis or interpretation of data |
| **Selina Leber, MS** | University of Basel | Analysis or interpretation of data |
| **Charidimos Tsagkas, MD, PhD** | University Hospital Basel, University of Basel | Drafting/revision of the manuscript for content, including medical writing for content |
| **Muhamed Barakovic, PhD** | University of Basel | Analysis or interpretation of data |
| **Riccardo Galbusera, MD** | University of Basel | Analysis or interpretation of data |
| **Po-Jui Lu, PhD** | University of Basel | Analysis or interpretation of data |
| **Matthias Weigel, PhD** | University of Basel | Drafting/revision of the manuscript for content, including medical writing for content |
| **Esther Ruberte, PhD** | University of Basel | Analysis or interpretation of data |
| **Ernst-Wilhelm Radue, MD** | University Hospital Basel | Drafting/revision of the manuscript for content, including medical writing for content |
| **Özgür Yaldizli, MD** | University Hospital Basel | Drafting/revision of the manuscript for content, including medical writing for content |
| **Johanna Oechtering, MD** | University Hospital Basel | Drafting/revision of the manuscript for content, including medical writing for content |
| **Johannes Lorscheider, MD** | University Hospital Basel | Drafting/revision of the manuscript for content, including medical writing for content |
| **Marcus D'Souza, MD** | University Hospital Basel | Drafting/revision of the manuscript for content, including medical writing for content |
| **Bettina Fischer-Barnicol, MD** | University of Basel | Drafting/revision of the manuscript for content, including medical writing for content |
| **Stefanie Müller, MD** | Cantonal Hospital St. Gallen | Drafting/revision of the manuscript for content, including medical writing for content |
| **Lutz Achtnichts, MD** | Cantonal Hospital Aarau | Drafting/revision of the manuscript for content, including medical writing for content |
| **Jochen Vehoff, MD** | Cantonal Hospital St. Gallen | Drafting/revision of the manuscript for content, including medical writing for content |
| **Giulio Disanto, MD, PhD** | Neurocenter of Southern Switzerland | Drafting/revision of the manuscript for content, including medical writing for content |
| **Oliver Findling, MD** | Kantonsspital Aarau | Drafting/revision of the manuscript for content, including medical writing for content |
| **Andrew Chan, MD** | Bern University Hospital, University of Bern | Drafting/revision of the manuscript for content, including medical writing for content |
| **Anke Salmen, MD** | Inselspital, Bern University Hospital | Drafting/revision of the manuscript for content, including medical writing for content |
| **Caroline Pot, MD, PhD** | Lausanne University Hospital | Drafting/revision of the manuscript for content, including medical writing for content |

## Appendix *(continued)*

| Name | Location | Contribution |
|---|---|---|
| **Claire Bridel, MD** | Hôpitaux Universitaires de Genève | Drafting/revision of the manuscript for content, including medical writing for content |
| **Chiara Zecca, MD** | Ospedale Clvico Lugano | Drafting/revision of the manuscript for content, including medical writing for content |
| **Tobias Derfuss, MD** | University Hospital Basel | Drafting/revision of the manuscript for content, including medical writing for content |
| **Johanna M. Lieb, MD** | University Hospital Basel, University of Basel | Drafting/revision of the manuscript for content, including medical writing for content |
| **Luca Remonda, MD** | Cantonal Hospital Aarau | Drafting/revision of the manuscript for content, including medical writing for content |
| **Franca Wagner, MD** | Department Diagnostic and Interventional Neuroradiology, University Hospital of Bern | Drafting/revision of the manuscript for content, including medical writing for content |
| **Maria Isabel Vargas, MD** | Geneva Hospital and University of Geneva | Drafting/revision of the manuscript for content, including medical writing for content |
| **Renaud A. Du Pasquier, MD** | Lausanne University Hospital | Drafting/revision of the manuscript for content, including medical writing for content |
| **Patrice H. Lalive, MD** | Geneva University Hospitals and Faculty of Medicine | Drafting/revision of the manuscript for content, including medical writing for content |
| **Emanuele Pravatà, MD** | Neurocenter of Southern Switzerland | Drafting/revision of the manuscript for content, including medical writing for content |
| **Johannes Weber, MD** | Institute of Radiology | Drafting/revision of the manuscript for content, including medical writing for content |
| **Philippe C. Cattin, PhD** | University of Basel | Drafting/revision of the manuscript for content, including medical writing for content |
| **Martina Absinta, MD, PhD** | Vita-Salute San Raffaele University and Hospital | Drafting/revision of the manuscript for content, including medical writing for content; analysis or interpretation of data |
| **Claudio Gobbi, MD** | Ospedale Regionale di Lugano | Drafting/revision of the manuscript for content, including medical writing for content |
| **David Leppert, MD** | University Hospital Basel | Drafting/revision of the manuscript for content, including medical writing for content |
| **Ludwig Kappos, MD** | University Hospital Basel | Drafting/revision of the manuscript for content, including medical writing for content |
| **Jens Kuhle, MD, PhD** | University Hospital Basel | Drafting/revision of the manuscript for content, including medical writing for content; major role in the acquisition of data; study concept or design; analysis or interpretation of data |
| **Cristina Granziera, MD, PhD** | University Hospital Basel | Drafting/revision of the manuscript for content, including medical writing for content; major role in the acquisition of data; study concept or design; analysis or interpretation of data |

## References


1. Kobelt G, Thompson A, Berg J, Gannedahl M, Eriksson J. New insights into the burden and costs of multiple sclerosis in Europe. *Mult Scler*. 2017;23(8):1123-1136. doi:10.1177/1352458517694432
2. Lublin FD, Reingold SC, Cohen JA, et al. Defining the clinical course of multiple sclerosis: the 2013 revisions. *Neurology*. 2014;83(3):278-286. doi:10.1212/WNL.0000000000000560
3. Kappos L, Butzkueven H, Wiendl H, et al. Greater sensitivity to multiple sclerosis disability worsening and progression events using a roving versus a fixed reference value in a prospective cohort study. *Mult Scler J*. 2018;24(7):963-973. doi:10.1177/1352458517709619
4. Kappos L, Wolinsky JS, Giovannoni G, et al. Contribution of relapse-independent progression vs relapse-associated worsening to overall confirmed disability accumulation in typical relapsing multiple sclerosis in a pooled analysis of 2 randomized clinical trials. *JAMA Neurol*. 2020;77(9):1132-1140. doi:10.1001/jamaneurol.2020.1568
5. Cree BAC, Hollenbach JA, Bove R, et al. Silent progression in disease activity–free relapsing multiple sclerosis. *Ann Neurol*. 2019;85(5):653-666. doi:10.1002/ana.25463
6. Lublin FD, Häring DA, Ganjgahi H, et al. How patients with multiple sclerosis acquire disability. *Brain*. 2022;145(9):3147-3161. doi:10.1093/brain/awac016
7. Cagol A, Schaedelin S, Barakovic M, et al. Association of brain atrophy with disease progression independent of relapse activity in patients with relapsing multiple sclerosis. *JAMA Neurol*. 2022;79(7):682-692. doi:10.1001/jamaneurol.2022.1025
8. Tsagkas C, Magon S, Gaetano L, et al. Spinal cord volume loss: a marker of disease progression in multiple sclerosis. *Neurology*. 2018;91(4):e349-e358. doi:10.1212/WNL.0000000000005853
9. Lukas C, Knol DL, Sombekke MH, et al. Cervical spinal cord volume loss is related to clinical disability progression in multiple sclerosis. *J Neurol Neurosurg Psychiatry*. 2015;86(4):410-418. doi:10.1136/JNNP-2014-308021
10. Bischof A, Papinutto N, Keshavan A, et al. Spinal cord atrophy predicts progressive disease in relapsing multiple sclerosis. *Ann Neurol*. 2022;91(2):268-281. doi:10.1002/ana.26281
11. Frischer JM, Weigand SD, Guo Y, et al. Clinical and pathological insights into the dynamic nature of the white matter multiple sclerosis plaque. *Ann Neurol*. 2015;78(5):710-721. doi:10.1002/ana.24497
12. Dal-Bianco A, Grabner G, Kronnerwetter C, et al. Slow expansion of multiple sclerosis iron rim lesions: pathology and 7 T magnetic resonance imaging. *Acta Neuropathol*. 2017;133(1):25. doi:10.1007/S00401-016-1636-Z
13. Absinta M, Sati P, Masuzzo F, et al. Association of chronic active multiple sclerosis lesions with disability in vivo. *JAMA Neurol*. 2019;76(12):1474. doi:10.1001/JAMANEUROL.2019.2399
14. Disanto G, Benkert P, Lorscheider J, et al. The Swiss Multiple Sclerosis Cohort-Study (SMSC): a prospective Swiss wide investigation of key phases in disease evolution and new treatment options. *PLoS One*. 2016;11(3):e0152347. doi:10.1371/journal.pone.0152347
15. Thompson AJ, Banwell BL, Barkhof F, et al. Diagnosis of multiple sclerosis: 2017 revisions of the McDonald criteria. *Lancet Neurol*. 2018;17(2):162-173. doi:10.1016/S1474-4422(17)30470-2
16. Von Elm E, Altman DG, Egger M, Pocock SJ, Gøtzsche PC, Vandenbrouckef JP. The Strengthening the Reporting of Observational Studies in Epidemiology (STROBE) statement: guidelines for reporting observational studies. *Bull World Health Organ*. 2007;85(11):867-872. doi:10.2471/BLT.07.045120
17. Kurtzke JF. Rating neurologic impairment in multiple sclerosis: an expanded disability status scale (EDSS). *Neurology*. 1983;33(11):1444-1452. doi:10.1212/wnl.33.11.1444
18. Accessed January 10, 2023. neurostatus.net/.

19. Andermatt S, Pezold S, Cattin PC. Automated segmentation of multiple sclerosis lesions using multi-dimensional gated recurrent units. In: *Lecture Notes in Computer Science (Including Subseries Lecture Notes in Artificial Intelligence and Lecture Notes in Bioinformatics). Vol. 10670 LNCS*. Springer; 2018:31-42. doi:10.1007/978-3-319-75238-9_3
20. Fartaria MJ, Kober T, Granziera C, Bach Cuadra M. Longitudinal analysis of white matter and cortical lesions in multiple sclerosis. *Neuroimage Clin*. 2019;23:101938. doi:10.1016/j.nicl.2019.101938
21. De Leener B, Cohen-Adad J, Kadoury S. Automatic segmentation of the spinal cord and spinal canal coupled with vertebral labeling. *IEEE Trans Med Imaging*. 2015;34(8):1705-1718. doi:10.1109/TMI.2015.2437192
22. Puonti O, Iglesias JE, Van Leemput K. Fast and sequence-adaptive whole-brain segmentation using parametric Bayesian modeling. *Neuroimage*. 2016;143:235-249. doi:10.1016/j.neuroimage.2016.09.011
23. Liu T, Xu W, Spincemaille P, Avestimehr AS, Wang Y. Accuracy of the morphology enabled dipole inversion (MEDI) algorithm for quantitative susceptibility mapping in MRI. *IEEE Trans Med Imaging*. 2012;31(3):816-824. doi:10.1109/TMI.2011.2182523
24. *R: Version 4.2.1*. R Core Team; 2022. Accessed January 10, 2023. R-project.org.
25. Bernal-Rusiel JL, Greve DN, Reuter M, Fischl B, Sabuncu MR. Statistical analysis of longitudinal neuroimage data with linear mixed effects models. *Neuroimage*. 2013;66:249-260. doi:10.1016/j.neuroimage.2012.10.065
26. Maggi P, Kuhle J, Schädelin S, et al. Chronic white matter inflammation and serum neurofilament levels in multiple sclerosis. *Neurology*. 2021;97(6):e543-e553. doi:10.1212/WNL.0000000000012326
27. Shrout PE, Fleiss JL. Intraclass correlations: uses in assessing rater reliability. *Psychol Bull*. 1979;86(2):420-428. doi:10.1037//0033-2909.86.2.420
28. Kearney H, Miller DH, Ciccarelli O. Spinal cord MRI in multiple sclerosis-diagnostic, prognostic and clinical value. *Nat Rev Neurol*. 2015;11(6):327-338. doi:10.1038/nrneurol.2015.80
29. Biberacher V, Boucard CC, Schmidt P, et al. Atrophy and structural variability of the upper cervical cord in early multiple sclerosis. *Mult Scler*. 2015;21(7):875-884. doi:10.1177/1352458514546514
30. Casserly C, Seyman EE, Alcaide-Leon P, et al. Spinal cord atrophy in multiple sclerosis: a systematic review and meta-analysis. *J Neuroimaging*. 2018;28(6):556-586. doi:10.1111/jon.12553
31. Sastre-Garriga J, Pareto D, Battaglini M, et al. MAGNIMS consensus recommendations on the use of brain and spinal cord atrophy measures in clinical practice. *Nat Rev Neurol*. 2020;16(3):171-182. doi:10.1038/s41582-020-0314-x
32. Losseff NA, Webb SL, O'Riordan JI, et al. Spinal cord atrophy and disability in multiple sclerosis. A new reproducible and sensitive MRI method with potential to monitor disease progression. *Brain*. 1996;119(3):701-708. doi:10.1093/brain/119.3.701
33. Rocca MA, Horsfield MA, Sala S, et al. A multicenter assessment of cervical cord atrophy among MS clinical phenotypes. *Neurology*. 2011;76(24):2096-2102. doi:10.1212/WNL.0b013e31821f46b8
34. Azevedo CJ, Cen SY, Khadka S, et al. Thalamic atrophy in multiple sclerosis: a magnetic resonance imaging marker of neurodegeneration throughout disease. *Ann Neurol*. 2018;83(2):223-234. doi:10.1002/ana.25150
35. Pagani E, Rocca MA, Gallo A, et al. Regional brain atrophy evolves differently in patients with multiple sclerosis according to clinical phenotype. *Am J Neuroradiol*. 2005;26(2):341-346.
36. Eijlers AJC, Dekker I, Steenwijk MD, et al. Cortical atrophy accelerates as cognitive decline worsens in multiple sclerosis. *Neurology*. 2019;93(14):E1348-E1359. doi:10.1212/WNL.0000000000008198
37. Sastre-Garriga J, Pareto D, Rovira À. Brain atrophy in multiple sclerosis: clinical relevance and technical aspects. *Neuroimaging Clin N Am*. 2017;27(2):289-300. doi:10.1016/j.nic.2017.01.002
38. Martire MS, Moiola L, Rocca MA, Filippi M, Absinta M. What is the potential of paramagnetic rim lesions as diagnostic indicators in multiple sclerosis? *Expert Rev Neurother*. 2022;22(10):829-837. doi:10.1080/14737175.2022.2143265
39. Kwong KCNK, Mollison D, Meijboom R, et al. The prevalence of paramagnetic rim lesions in multiple sclerosis: a systematic review and meta-analysis. *PLoS One*. 2021;16(9):e0256845. doi:10.1371/journal.pone.0256845
40. Luchetti S, Fransen NL, van Eden CG, Ramaglia V, Mason M, Huitinga I. Progressive multiple sclerosis patients show substantial lesion activity that correlates with clinical disease severity and sex: a retrospective autopsy cohort analysis. *Acta Neuropathol*. 2018;135(4):511-528. doi:10.1007/s00401-018-1818-y
41. Marcille M, Hurtado Rúa S, Tyshkov C, et al. Disease correlates of rim lesions on quantitative susceptibility mapping in multiple sclerosis. *Sci Rep*. 2022;12(1):4411. doi:10.1038/s41598-022-08477-6
42. Trapp BD, Peterson J, Ransohoff RM, Rudick R, Mörk S, Bö L. Axonal transection in the lesions of multiple sclerosis. *N Engl J Med*. 1998;338(5):278-285. doi:10.1056/nejm199801293380502
43. Correale J, Gaitán MI, Ysrraelit MC, Fiol MP. Progressive multiple sclerosis: from pathogenic mechanisms to treatment. *Brain*. 2017;140(3):527-546. doi:10.1093/BRAIN/AWW258
44. Altokhis AI, Hibbert AM, Allen CM, et al. Longitudinal clinical study of patients with iron rim lesions in multiple sclerosis. *Mult Scler J*. 2022;28(14):2202-2211. doi:10.1177/13524585221114750
45. Hemond CC, Reich DS, Dundamadappa SK. Paramagnetic rim lesions in multiple sclerosis: comparison of visualization at 1.5-T and 3-T MRI. *Am J Roentgenol*. 2022;219(1):120-129. doi:10.2214/AJR.21.26777
46. Bian W, Harter K, Hammond-Rosenbluth KE, et al. A serial in vivo 7T magnetic resonance phase imaging study of white matter lesions in multiple sclerosis. *Mult Scler*. 2013;19(1):69-75. doi:10.1177/1352458512447870
47. Absinta M, Sati P, Fechner A, Schindler MK, Nair G, Reich DS. Identification of chronic active multiple sclerosis lesions on 3T MRI. *Am J Neuroradiol*. 2018;39(7):1233-1238. doi:10.3174/ajnr.A5660
48. Bsteh G, Hegen H, Altmann P, et al. Retinal layer thinning is reflecting disability progression independent of relapse activity in multiple sclerosis. *Mult Scler J Exp Transl Clin*. 2020;6(4):2055217320966344. doi:10.1177/2055217320966344
49. Portaccio E, Bellinvia A, Fonderico M, et al. Progression is independent of relapse activity in early multiple sclerosis: a real-life cohort study. *Brain*. 2022;145(8):2796-2805. doi:10.1093/brain/awac111